The Online ANGLE ORTHODONTIST
An International Journal of Orthodontics and Dentofacial Orthopedics
78th Anniversary 1930–2008

HOME | CURRENT ISSUE | FUTURE ISSUES | PAST ISSUES | SEARCH | ANGLE SOCIETY | RELATED LINKS

Proudly Sponsored by *The EH Angle Education and Research Foundation*

[**Print Version**]
[**PubMed Citation**] [**Related Articles in PubMed**]

TABLE OF CONTENTS

Regenerate Bone Formation and Remodeling During Mandibular Osteodistraction

Jason B. Cope, DDS, PhD;[a] Mikhail L. Samchukov, MD[b]

ABSTRACT

The purpose of this study was to evaluate the newly formed bone during the consolidation period of mandibular osteodistraction using quantitative histology. Seventeen skeletally mature conditioned male beagle dogs underwent 10 mm of bilateral mandibular lengthening. After distraction, the regenerates were allowed to consolidate for 0, 2, 4, 6, or 8 weeks, at which time the animals were sacrificed and tissues harvested for standard histologic and histomorphometric analyses. Mineralization began at the host bone margins by the end of the distraction period, followed by a progressive increase in trabecular bone, with a concomitant decrease in the amount of fibrous tissue. Between 4 to 6 weeks of consolidation, 3 types of relatively mature distraction regenerates were evident. The mineral apposition rate gradually increased from the end of distraction to the fourth week of consolidation, at which time it remained constant until sometime before the eighth week, when it tapered off slightly as remodeling increased.

KEY WORDS: Distraction osteogenesis, Consolidation, Mandible, Histomorphometry, Mineral apposition rate.

Accepted: January 2000. Submitted: August 1999.

INTRODUCTION Return to TOC

The consolidation period is one of the most important phases of distraction osteogenesis. During this period, the newly formed collagenous tissue mineralizes to form parallel oriented bony trabeculae within the distraction gap. Remodeling of this woven bone begins simultaneously at the host bone margins. Although the application of craniofacial distraction osteogenesis has dramatically increased in the last decade; the specific details of new bone formation and remodeling are still disputed.

Regenerate tissue mineralization and remodeling has been investigated experimentally by several authors, mainly by radiography,[1–4] ultrasound,[5,6] computed tomography,[7–9] light microscopy,[10–14] and electron microscopy.[15–17] Although histologic evaluation is limited to human biopsy material or to tissues harvested at the endpoint of animal experiments, it is the only method by which to directly visualize all tissue components, as well as their spatial relationships to one another. Moreover, direct quantification of cell and matrix types, and bone formation rates are possible.

Quantitative histology has been used for years in limb lengthening to assess mineralization dynamics and remodeling of distraction regenerate bone,[18–20] yet it has not been reported to assess these parameters in craniofacial distraction osteogenesis. Therefore, the

purpose of this study was to evaluate by quantitative histology, the newly formed bone during the consolidation period of mandibular osteodistraction. The hypothesis to be tested was that mineralization of the newly formed bone during mandibular distraction osteogenesis does not occur at a constant rate. Rather, mineralization gradually increases and peaks between 2 to 4 weeks, then tapers off as remodeling increases. Total trabecular bone area, however, does progressively increase at all time points during the consolidation period.

MATERIALS AND METHODS [Return to TOC]

Animal model

Seventeen skeletally mature conditioned male beagle dogs weighing 10 to 15 kg were used in this study. Except for untreated controls (n = 5), all dogs underwent 10 mm of bilateral mandibular lengthening via our previously described intraoral distraction osteogenesis technique.[3,4,7] Briefly, while preserving the mandibular nerve, bilateral midbody osteotomies were performed between the mandibular third and fourth premolars followed by placement of intraoral bone-borne distraction devices ([Figure 1] ⊙). After a latency period of 7 days, activation of the devices began at a rate of 0.5 mm twice a day for 10 days, followed by a consolidation period of either 0 (n = 1), 2 (n = 1), 4 (n = 4), 6 (n = 4), or 8 weeks (n = 2). During the study, each animal was given 25 mg/kg intravenous tetracycline HCl (Sigma, St Louis, Mo) and 10 mg/kg intravenous calcein (Sigma) as vital bone labels, 14 days and 2 days prior to sacrifice, respectively. Following consolidation, the animals were sacrificed using intravenous sodium pentobarbital (100 mg/kg). The housing, care, and experimental protocol were in accordance with the guidelines set forth by the TAMUS-Baylor College of Dentistry Institutional Animal Care and Use Committee.

Tissue processing

At necropsy, the mandibles were resected en bloc, then hemisected through the fibrous symphysis and randomly assigned for either standard histologic analysis or histomorphometry. The hemimandibles designated for standard histology were trimmed to encompass the area of regenerate bone including at least 2.5 mm of host bone proximal and distal to the regenerate, then sagittally hemisected and fixed for 1 week in 10% neutral buffered formalin. Following fixation, the specimens were rinsed in distilled water and decalcified with 0.5 M Ethylenediamine tetra acetic acid (EDTA) (pH 7.4), at which time the specimens were continuously dehydrated through an ascending ethanol series and paraffin embedded. Consecutively numbered serial sagittal sections (6 μm thick) were cut through the full thickness of each specimen. The first 2 slides of every series were then stained with Harris' hematoxylin and eosin (H & E)[21] and a modified Attwood's stain,[22] respectively. The H & E slides were used for standard histologic description. The Attwood's stained slides were used to calculate the percent distribution of the 3 major extracellular matrices within the regenerate—bone, fibrous tissue, or cartilage.
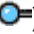
The remaining hemimandibles were trimmed in the same way and fixed in 70% ethanol for 1 week. The samples were then processed and embedded in methylmethacrylate, sectioned, precision mounted on acrylic sheets, and ground to a thickness of 20–30 μm on an Exakt Cutting-Grinding System (Exakt, Hamburg, Germany). Two sections of each mandible were stained for 10 minutes with Sanderson's Rapid Bone Stain (Surgipath Medical Industries Inc, Richmond, Ill) for histomorphometric analysis.[23] The first section was used to analyze the vital bone labels. The second section was counterstained with Van Gieson's solution as described by Sanderson.[23] This counterstain provides high contrast between bone, cartilage, fibrous tissue, and marrow in order to use the threshold method[24] for quantifying trabecular bone area.

Histomorphologic quantification

Using a ScanMaker 4 flatbed scanner (Microtek Labs Inc, Redondo Beach, Cal), the Attwood's stained slides were digitized as 24-bit color images at a resolution of 600 × 1200 dpi and saved as TIFF images using a lossless LZW compression algorithm on a Pentium PC. Prior to digitization, the scanner was calibrated for accuracy using an Agfa IT8.7/1 gray scale target (Agfa-Gevaert N.V., Mortsel, Belgium) and standard protocols.[25,26] After image acquisition, the files were transferred to Metamorph Imaging System v4.0 (Universal Imaging Corp, West Chester, Penn), which had been previously calibrated with a Nikon 0.01 mm Objective Micrometer (model MBM11100, Nikon Corp, Japan). Once in Metamorph, the percent contribution of each tissue relative to the total regenerate was obtained by tracing a region of interest (ROI) around each tissue component (bone, fibrous tissue, or cartilage). All measurements were logged to a spreadsheet for analysis.

Histomorphometric analysis

The Van Gieson's stained slides were digitized as described above. The Sanderson's stained slides were captured at a magnification of 40× via a MicroMAX black and white scientific digital camera (model RTE/CCC-732-Y, Princeton Instruments Inc, Trenton, NJ) coupled to a Nikon Labophot brightfield microscope (Nikon Corp, Japan) with a Nikon Super High Pressure Mercury Lamp (model LH-M100CB–1, Nikon Corp, Japan) for epifluorescence. On each image, a grid containing 3 horizontal rows (crestal, central, and cortical) of 7 ROIs each (area = 2.27 mm^2) was placed over the distal host bone, distal regenerate, middle distal regenerate, interzone, middle proximal regenerate, proximal regenerate, and proximal host bone, for a total of 21 ROIs on each section ([Figure 2] ⊙). The 18 ROIs in the regenerate represented approximately 33% of the total regenerate area.

Since the digital camera was black and white, the capture of fluorescent images demonstrating both tetracycline and calcein was accomplished in 2 stages. Initially, each slide was captured twice as a grayscale TIFF image using lossless compression. The first image was captured using a Dapi (405 nm) filter to produce an image with tetracycline emitting the brightest light. The second image was captured using a Fitc (490 nm) filter to produce an image with calcein emitting the brightest light. Each set of 2 images was then superimposed and color encoded into 1 image, the first being encoded in the green channel and the second in the red channel, to produce 1 image demonstrating tetracycline as green and calcein as orange (Figure 3 ⊙=).

Two measurement methods were used—direct object tracing (regenerate height and width, trabecular length and width, and interlabel distance) and image thresholding (trabecular bone area). Briefly, color image thresholding allows the operator to select a range of specific colors (in this case, the shades of red staining the trabecular bone). The total surface area of this color range is then automatically calculated by the software. Interlabel distance, which gives the mineral apposition rate when divided by the number of days between injections, was measured from the midpoint of the first label to the midpoint of the second label. At least 20 interlabel distances were measured for every ROI, and all interlabel lines were drawn perpendicular to the tangent of the label. Measurement data was then logged to a spreadsheet for analysis.

Statistical analysis

The histomorphometric results were evaluated using repeated measures analysis of variance (ANOVA) with profile testing. When missing data precluded a meaningful repeated measures ANOVA, the results were evaluated using an unbalanced 2-way ANOVA without interaction in which Animal and Site were the 2 factors. If significant differences were seen, Tukey multiple comparison procedures were used to identify the differences. Comparisons between 2 sites on the same animal were performed using the paired t-test. When comparing the same site for 2 different time periods, the 2-sample t-test assuming unequal variances was used. The significance level was set at $P < .05$. All results are given as mean values ± standard deviation.

RESULTS

Control

As expected, only bone was seen in the untreated control group. The total bone area varied between the regions. Crestal and cortical regions had significantly more ($P < .03$) trabecular bone than central regions (Table 1 ⊙=). Likewise, less marrow space was seen for these regions with densely packed trabeculae. Both the tetracycline and calcein bone labels were distinctly visible within the control bone, giving an average mineral apposition rate (MAR) for all 6 regions of 1.99 ± 0.6 μm/day (Table 2 ⊙=).

Zero weeks

Immediately following completion of 10 mm of bilateral mandibular distraction, histologic examination revealed a distraction gap filled with fibrovascular tissue comprising 70% to 93% of the total regenerate area and organized as parallel arranged collagen bundles with interspersed vascular channels. No evidence of cartilage tissue was seen in the distraction gap. At this time point, both regenerates demonstrated some evidence of new bone formation. Only 2% to 5% of the regenerate consisted of bony trabeculae; the remaining 4% to 27% was marrow space. The areas of new bone formation were visualized as triangular shaped regions of ossification with the base at the host bone margins and the apex projecting into the distraction gap (Figure 4 ⊙=). The trabeculae within the regenerate were oriented parallel to the direction of distraction and averaged 394 ± 182 μm in length and 103 ± 39 μm thickness. The majority of trabeculae originated adjacent to the inferior alveolar canal, however, small areas of new bone formation were also found adjacent to the inferior cortex. The bony trabeculae in this area were not oriented parallel to the direction of distraction, but instead looked like the typical hard fracture callus.

Analysis of the individual 2.27 mm^2 ROIs revealed a distinct appearance of both bone labels only at the host bone margin in the crestal proximal regenerate (ROI 16). The MAR in this region was 1.83 μm/day. Within the host bone, however, the MAR was above 2 μm/day for all 6 ROIs (Table 2 ⊙=).

Two weeks

At 2 weeks of consolidation, the histomorphologic appearance of the areas of new bone formation within the regenerate varied both in terms of amount and location. Some sections looked similar to the zero-week distraction regenerates with small areas of new bone formation located at the host bone margins (Figure 5A ⊙=). Others had regions of bony trabeculae extending up to half the total width of the distraction gap from each host bone margin, such that the fibrous interzone in some areas was less than 2 mm (Figure 5B ⊙=). The linearly oriented bony trabeculae averaged 1324 ± 732 μm in length and 152 ± 55 μm thickness. No evidence of cartilage tissue was seen. The areas of hard callus adjacent to the inferior cortex increased slightly in size.

Evaluation of the individual ROIs demonstrated that bony trabeculae occupied up to 20.37% in the crestal, 35.39% in the central, and 2.31% in the cortical ROIs (Table 1 ⊙=). Although not statistically significant, an apparent difference existed between the regenerate regions adjacent to the proximal vs the distal host bone segments, particularly in the crestal and central regions. In the crestal and central

regions, the average trabecular bone area of the proximal and middle proximal ROIs was 22.24% ± 10.12%, whereas this value was only 9.21% ± 10.01% for the distal and middle distal regions. Two distinct labels were visible only in the proximal and distal ROIs. In these regions, the MAR ranged from 1.30–2.78 μm/day. The MAR of the host bone decreased relative to the zero-week regenerate, as only 2 of 6 regions were over 2 μm/day (Table 2 ⊙).

Four weeks

Between 4 to 6 weeks of consolidation, 3 histologically distinct types of regenerate were evident, demonstrating the progression of regenerate maturation (Figure 6 ⊙). Two were initially seen at 4 weeks and the other at 6 weeks. At 4 weeks of consolidation, the Type I regenerate (n = 5) had a wide fibrous interzone (3.7 ± 2.2 mm) that extended the entire height of the regenerate (Figure 7A ⊙). The interzone was bounded on either side by marrow space (29% ± 5%) and bony trabeculae (43% ± 8%) that originated from the host bone margins. The linearly oriented trabeculae averaged 1152 ± 376 μm in length and 222 ± 95 μm thickness. The Type III regenerate (n = 4) was characterized by varying degrees of interzone obliteration (Figure 7B ⊙). Where an interzone was present, it was more narrow (2.5 ± 1.4 mm) than the Type I regenerate. For these regenerates, bone trabeculae occupied 61% ± 7% of the total regenerate, while 23% ± 6% was marrow space. The linearly oriented trabeculae averaged 2218 ± 1197 μm in length and 251 ± 134 μm thickness.

The majority of regenerates at 4 weeks of consolidation had small islands of cartilage tissue (2% to 4% regenerate area). The chondrocytes were arranged in an irregular pattern with no clearly defined cellular orientation; there was no apparent progression from proliferation to hypertrophy. There was also a relative paucity of invading capillaries at the edges of the cartilage. Regardless of regenerate type, all islands of cartilage were found in close proximity to the mandibular nerve, either slightly inferior or superior to the inferior alveolar canal. The size of the hard callus formed adjacent to the inferior cortex was similar to the 2-week consolidation regenerates.

At this time point, newly formed bone was visible in every ROI of the regenerate. Again, a difference, although not statistically significant, was seen between the regenerate regions adjacent to the proximal vs the distal host bone segments, particularly in the crestal and central regions (Table 1 ⊙). In the crestal and central regions, the average trabecular bone area of the proximal ROIs was 39.48% ± 22.08%, whereas this value was only 25.50% ± 12.75% for the distal regions. The proximal and distal cortical ROIs, as well as ROIs 7–15 (middle portion of regenerate), demonstrated no difference in trabecular bone area. In this group, 2 distinct bone labels were visible in every ROI throughout the regenerate with a mean MAR of 2.67 ± 0.36 μm/day (Table 2 ⊙). The MAR of the host bone at 4 weeks increased relative to the 2-week value, although the increase was not statistically significant.

Six weeks

By 6 weeks of consolidation, the Type II regenerate (n = 2) was evident. It was characterized by a dissimilar appearance of the interzone above and below the mandibular nerve (Figure 8 ⊙). The interzone superior to the mandibular nerve was predominantly fibrous and moderately wide (5.1 ± 2.8 mm). The interzone inferior to the mandibular nerve was mostly obliterated, narrow when present (0.73 ± 0.69 mm), and often filled with cartilage tissue. For this regenerate, trabecular bone occupied 45% ± 5% of the regenerate, with marrow space occupying 39% ± 12%. Fibrous and cartilage tissue occupied only 13% ± 4% and 2% ± 1% of the total regenerate, respectively.

Both regenerate Types I and III (n = 1 and 5, respectively) were also present with a percent distribution of bone, marrow, fibrous, and cartilage tissues similar to the 4-week values (60% ± 3%, 29% ± 5%, 14% ± 3%, and 2% ± 0.5%, respectively). The linearly oriented primary bony trabeculae for all of the 6-week regenerates averaged 2437 ± 1294 μm in length and 195 ± 85 μm thickness. The amount of hard callus seen adjacent to the inferior cortex was similar to that of the previous consolidation period.

At this point of consolidation, no difference was seen between the proximal and distal regenerate ROIs for either trabecular bone or MAR. However, consistent patterns were evident with regard to the amount of bone within the vertically oriented regions of interest (Table 1 ⊙). The trabecular bone in the cortical ROIs (66.92% ± 11.01%) was significantly greater (P = .02) than that of the central (47.07% ± 10.59%) or crestal (40.66% ± 7.45%) ROIs. In addition, the amount of trabecular bone progressively increased from the outer vertical regions of the regenerate toward the interzone ROIs, giving a P-value of 0.06. Comparing the contiguous vertical ROIs in the regenerate, significantly more (P < .04) trabecular bone was seen in the middle distal ROIs than in the interzone ROIs. The MAR in this group was similar to the 4-week group, averaging 2.76 ± 0.46 μm/day. The host bone MAR was slightly lower than the 4-week value, but the difference was not significant (Table 2 ⊙).

Eight weeks

The regenerates evaluated after a consolidation period of 8 weeks demonstrated a further progression of bone formation, with several having almost complete obliteration of the interzone (Figure 9 ⊙). In fact, if cartilage tissue had not been present in the middle of some regenerates, it would have been difficult to determine the approximate location of the interzone. The percent contribution of each tissue type relative to the total regenerate area, as well as the trabecular lengths and widths, were similar to those seen for the 4- and 6-week groups. The amount of hard callus seen adjacent to the inferior cortex decreased when compared to the previous consolidation period.

The trabecular bone in the 8-week proximal and distal regenerate regions (44.99% ± 17.60%) was greater than that at 6 weeks of consolidation (40.86% ± 15.97%) (Table 1 ⊙). Comparisons of these values indicate a trend toward significance (P = .06). The MAR in this group was lower than the 4- or 6-week group, averaging only 2.34 ± 0.31 μm/day (Table 2 ⊙). The host bone MAR also decreased to

an average of 1.86 ± 0.58 μm/day.

DISCUSSION [Return to TOC]

The application of distraction osteogenesis to the craniofacial skeleton has the potential to greatly enhance our ability to treat both complex and routine surgical patients. However, due to the relatively short history of the technique in the maxillofacial area, little experimental data has been presented with regard to the appropriate duration of the consolidation period prior to removal of the distraction device. This period is critical since premature device removal may lead to regenerate bending or fracture,[27] whereas prolonged consolidation may lead to stress shielding,[19,28] also potentially weakening the regenerate. It is therefore important to assess bone formation and remodeling during osteodistraction in order to better understand the influence of the consolidation period clinically.

The current study analyzed the dynamics of new bone formation during mandibular distraction osteogenesis. By demonstrating the presence of initial areas of mineralization at the beginning of the consolidation period, our results indicate that new bone formation during mandibular osteodistraction starts prior to the tenth day of distraction. This time-frame is within the range for limb lengthening (7–14 days after beginning distraction) previously reported by Aronson,[29] and others.[16,18,30–31]

The data suggests that the percent of new trabecular bone increased at all time points during the consolidation period. From zero to 8 weeks of consolidation, maturation of the regenerate tissue was characterized by a progressive increase in new bone, with a concomitant decrease in the amount of fibrous tissue. At the end of the distraction period, trabecular bone and marrow space occupied up to 5% and 27% of the total regenerate, respectively. The remainder of the regenerate consisted of fibrovascular tissue oriented parallel to the direction of distraction. With each subsequent 2-week interval, progressively more bone formed and less fibrous tissue was present within the distraction gap. Similar to the increase in trabecular bone during the consolidation period, the average trabecular length and thickness also increased progressively from zero to 8 weeks of consolidation.

Interestingly, 3 types of relatively mature regenerates were observed during consolidation. Type I corresponded to the classic 3 zonal regenerate seen as 2 mineralizing zones separated by an intervening fibrous interzone.[29] For the Type II regenerate, most of the crestal part of the interzone was present, but the central and cortical interzone areas were mostly obliterated. The Type III regenerate was characterized by almost complete obliteration of the interzone with few isolated islands of fibrous or cartilage tissue. Although these regenerate types were evident at different time periods, they likely represent a continuum of individual regenerate maturation. For example, the classic 3 zonal regenerate (Type I) may progress to a Type II regenerate with obliteration of the inferior aspect of the interzone, but with patency of the superior aspect of the interzone. The Type III regenerate would represent the last stage of regenerate maturation when interzone obliteration is almost complete and remodeling activities supercede bone formation.

Within the distraction regenerates studied, the membranous pathway was the predominant mechanism of new bone formation. Although some areas of cartilage were present within the regenerates, possibly indicating endochondral bone formation, no cartilage was seen within the distraction gap until the fourth week of consolidation. At this and every subsequent period, the total amount of cartilage within the distraction gap averaged 2% to 3%, which is consistent with findings in tibial lengthening.[32] A previously unreported finding, however, was the consistent location of cartilage relative to the mandibular nerve. This was most probably due to the extraosseous location of the nerve in long bones when compared to the intraosseous location in the mandible. Speculative reasons for the specific location of cartilage in this report include the potential release of neuropeptides from the nerve or the possibility that the area of cartilage formation lays within the neutral axis of the regenerate where tensile forces may be minimal.

It is difficult to determine the exact nature of this cartilage tissue (ie, whether it was part of the traditional endochondral bone formation pathway or due to some local environmental reasons). First, nonrigid bone segment fixation, either during fracture healing or distraction osteogenesis, may allow clinically significant bone segment mobility, leading to microvascular disruption and altered osteogenesis.[13,16,33] Second, the rate and rhythm at which the bone segments were distracted, although similar to current clinical and experimental protocols, could slightly exceed the growth capacity of the associated capillaries, also leading to decreased oxygen tension within the interzone.[34] Finally, an unconventional alternative has previously been presented by Yasui and colleagues[35] and supported by others.[36–38] It suggests that the presence of cartilage or chondroid tissue may actually be indicative of a third type of "transchondroid" bone formation in which cartilage forms, possibly due to decreased oxygen tension,[39] but is then directly transformed into bone rather than by the traditionally accepted endochondral pathway. This seems the most likely explanation since device fixation was clinically stable and the distraction rate and rhythm was similar to most other osteodistraction dog studies. The fact that no distinct pattern of chondrocyte differentiation was evident (ie, the normal progression from proliferation to hypertrophy followed by apoptosis and vascular invasion suggests that this may in fact be transchondroid bone and not typical endochondral ossification.) The lack of chondrocyte apoptosis was verified by a Tdt-mediated dUTP-biotin Nick End Labelling (TUNEL) assay and reported elsewhere.

The newly formed bone varied in terms of amount and location in all 3 dimensions. For example, at 2 and 4 weeks of consolidation, when bone formation was progressing rapidly, the amount of trabecular bone on the proximal side of the regenerate was at least 1.5 times higher than that of the distal side. This is not unexpected, however, and previous studies have reported similar findings of regenerate polarity.[40,41] Most speculate that increased vasculature proximal to the regenerate, probably stemming from the associated muscle bellies, causes the proximal to distal regenerate differences. Variances were also seen along the vertical height of the regenerate as illustrated by the Type II regenerate, in which much of the fibrous interzone was still present in the crestal regions. This is most probably due to an inadequate

amount of interradicular host bone on either side of the osteotomy in the crestal region, leading to a lag in crestal osteogenesis. Recently, Bell and colleagues[42,43] found similar results on baboons when accidentally exposing the periodontal ligament of mandibular incisors during midline widening. The cortical regions, on the other hand, where the host bone was relatively thick and without the presence of tooth roots, never had an osseous defect and was always the first place where the interzone was obliterated. Moreover, by 6 weeks this cortical region had consistently more bone formed than the central or crestal regions. Finally, discrepancies in regenerate bone consolidation were seen in the mediolateral direction. The fibrous interzone was usually wider and more extensive at the center than at either the medial or the lateral extents of the regenerate.

Previously, several authors have reported the use of vital bone labels for craniofacial osteodistraction.[12,43–46] Unfortunately, no quantitative mineralization data was presented in those reports. It therefore appears that this is the first report to present the mineral apposition rate for craniofacial distraction osteogenesis. The results presented herein indicate that bone formation gradually increased from the end of distraction to the fourth week of consolidation, at which time it remained constant until sometime before the eighth week, when it tapered off slightly as remodeling increased. For example, bone formation had progressed and was evident in most ROIs by 2 weeks of consolidation, but 2 distinct labels were not always obvious. The reason for this is that initially, the newly formed woven bone was laid down rapidly in haphazard patterns with a diffuse uptake of the bone label. Technically, this diffuse labeling could not be used for calculating MAR. This does demonstrate, however, the extreme rapidity with which the fibrous regenerate was converted to osteoid and subsequently mineralized as woven bone, and is similar to previous studies of limb lengthening.[19,47] In those regions where MAR was calculable, it ranged from a low of 1.3 μm/day to a high of 2.78 μm/day, illustrating both the variability and rapidity of mineralization within the regenerate.

By 4 weeks of consolidation, the average MAR was 2.67 μm/day. This was approximately equivalent to the highest level seen at 2 weeks, indicating a progressive increase in MAR from zero to 4 weeks. Windhager and coworkers[19] also found an increase in mineralization between 3 and 5 weeks of consolidation. Over the next 2 weeks (4 to 6 weeks), the MAR remained at the same level, then slightly decreased over the last 2 weeks (6 to 8 weeks), suggesting that mineralization was beginning to slow as remodeling increased. A possible increase in remodeling at this point is supported by the fact that the MAR of the 8-week proximal and distal regenerate regions were lower than the same regions at 4 and 6 weeks, and lower than the middle proximal, interzone, and middle distal regions of the 8-week group. Others have also shown increased remodeling activity of the regenerate immediately proximal and distal to the host bone segments at 8 weeks of consolidation.[44,48]

CONCLUSIONS Return to TOC

In conclusion, 3 relatively mature types of regenerate were evident during the consolidation period of bilateral mandibular osteodistraction. Although the total amount of bone formation seen in each type of regenerate varied, the final percentage of trabecular bone increased from zero to 8 weeks of consolidation. Mineralization began at the host bone margins at the end of distraction and progressively increased up to the fourth week of consolidation at which time it remained stable for the following 2 weeks. This decreased slightly from 6 to 8 weeks of consolidation, as remodeling became the predominant activity of the regenerate.

ACKNOWLEDGMENTS

REFERENCES Return to TOC

1. Rachmiel A, Jackson IT, Potparic Z, Laufer D. Midface advancement in sheep by gradual distraction: A 1-year follow-up study. *J Oral Maxillofac Surg.* 1995; 53:525–529. [PubMed Citation]

2. Gantous A, Phillips JH, Catton P, Holmberg D. Distraction osteogenesis in the irradiated canine mandible. *Plast Reconstr Surg.* 1994; 93:164–168.

3. Cope JB, Samchukov ML. Mineralization dynamics of regenerate bone during mandibular osteodistraction. *Int J Oral Maxillofac Surg.* In press.

4. Cope JB, Samchukov ML, Cherkashin AM, Wolford LM, Franco P. Biomechanics of mandibular distractor orientation: An animal model analysis. *J Oral Maxillofac Surg.* 1999; 57:952–964.

5. Carls PF, Schuknecht B, Sailer HF. The ossification of the distraction gap after mandibular distraction evaluated by CT and US [abstract 25]. Paris, France: Second International Congress on Cranial and Facial Bone Distraction Processes. 1999;

6. Eyres KS, Bell MJ, Kanis JA. Methods of assessing new bone formation during limb lengthening. Ultrasonography, dual energy X-ray

absorptiometry, and radiography compared. *J Bone Joint Surg Br.* 1993; 75:358–364. [PubMed Citation]

7. Smith SW, Sachdeva RC, Cope JB. Evaluation of the consolidation period during osteodistraction using computed tomography. *Am J Orthod Dentofacial Orthop.* 1999; 116:254–263. [PubMed Citation]

8. Smatt V, Gibeili Z, Rahmi H, Robin M, Vanzo L, Smatt Y. Alveolar mandibular reconstruction by axial vertical distraction osteogenesis and oncology. In: Diner PA, Vasquez MP, eds. *Second International Congress on Cranial and Facial Bone Distraction Processes.* Bologna: Monduzzi Editore SpA. 1999;125–130.

9. Roth DA, Gosain AK, McCarthy JG, Stracher MA, Lefton DR, Grayson BH. A CT scan technique for quantitative volumetric assessment of the mandible after distraction osteogenesis. *Plast Reconstr Surg.* 1997; 99:1237–1247. [PubMed Citation]

10. Cope JB, Harper RP, Samchukov ML. Experimental tooth movement through regenerate alveolar bone: a pilot study. *Am J Orthod Dentofacial Orthop.* 1999; 116:501–505.

11. Farhadieh RD, Dickinson R, Yu Y, Gianoutsos MP, Walsh W. The role of transforming growth factor-beta, insulin-like growth factor I, and basic fibroblast growth factor in distraction osteogenesis of the mandible. *J Craniofac Surg.* 1999; 10:80–86. [PubMed Citation]

12. Michieli S, Miotti B. Lengthening of mandibular body by gradual surgical-orthodontic distraction. *J Oral Surg.* 1977; 35:187–192. [PubMed Citation]

13. Komuro Y, Takato T, Harii K, Yonemara Y. The histologic analysis of distraction osteogenesis of the mandible in rabbits. *Plast Reconstr Surg.* 1994; 94:152–159. [PubMed Citation]

14. Karaharju-Suvanto T, Peltonen J, Kahri A, Karaharju EO. Distraction osteogenesis of the mandible. An experimental study on sheep. *Int J Oral Maxillofac Surg.* 1992; 21:118–121.

15. Tsunokuma M, Nosaka Y, Hayashi H. et al. Neovascularization during distraction osteogenesis of the mandible in dogs. In: Diner PA, Vasquez MP, eds. *Second International Congress on Cranial and Facial Bone Distraction Processes.* Bologna: Monduzzi Editore SpA. 1999;345–352.

16. Peltonen JI, Kahri AI, Lindberg LA, Heikkila PS, Karaharju EO, Aalto KA. Bone formation after distraction osteotomy of the radius in sheep. *Acta Orthop Scand.* 1992; 63:599–603. [PubMed Citation]

17. Karaharju EO, Aalto K, Kahri A, Lindberg LA, Kallio T, Karaharju-Suvanto T, Vauhkonen M, Peltonen J. Distraction bone healing. *Clin Orthop.* 1993; 297:38–43.

18. Welch RD, Birch JG, Makarov MR, Samchukov ML. Histomorphometry of distraction osteogenesis in a caprine tibial lengthening model. *J Bone Miner Res.* 1998; 13:1–9. [PubMed Citation]

19. Windhager R, Tsuboyama T, Siegl H, Groszschmidt K, Seidl G, Schneider B, Plenk H Jr. Effect of bone cylinder length on distraction osteogenesis in the rabbit tibia. *J Orthop Res.* 1995; 13:620–628. [PubMed Citation]

20. Aronson J, Good B, Stewart C, Harrison B, Harp J. Preliminary studies of mineralization during distraction osteogenesis. *Clin Orthop Rel Res.* 1990; 250:43–49.

21. Luna LG. *Routine staining procedures..* In: Luna LG, ed. Manual of Histologic Staining Methods of the Armed Forces Institute of Pathology. New York, NY: McGraw-Hill Book Company. 1968;32–46.

22. Hess JA, Villanueva AR. Differential staining of decalcified teeth and bones by modified Attwood's stain. *Lab Med.* 1983; 14:435–438.

23. Sanderson C, Bloebaum RD. Advances in the staining of ground section histology. *Tech Bull Histotech.* 1993; 23:1–3.

24. Russ JC. *Segmentation and thresholding..* In: Russ JC, ed. The image processing handbook. Boca Raton, Fla: CRC Press. 1994;347–406.

25. Knoll T, Hamburg M, Narayanan S, Parent S, Good D. Getting images into photoshop: Detecting color casts. In: Knoll Teal, ed. *Adobe Photoshop 5.0 Users Guide.* San Jose, Cal: Adobe Systems Incorporated. 1998;53–54.

26. Russ JC. Image measurements: brightness measurements. In: Russ JC, ed. *The Image Processing Handbook.* Boca Raton, Fla; CRC Press. 1995;482–486.

27. Aronson J. Experimental and clinical experience with distraction osteogenesis. *Cleft Palate Craniofacial J.* 1994; 31:473–482.

28. Aronson J, Harrison BH, Stewart CL, Harp JH, Jr. The histology of distraction osteogenesis using different external fixators. *Clin*

Orthop. 1989; 241:106–116.

29. Aronson J. The biology of distraction osteogenesis. In: Bianchi Miocchi A, Aronson J, eds. *Operative Principles of Ilizarov.* Baltimore, Md: Williams & Wilkins. 1991;42–52.

30. Delloye C, Delefortrie G, Coutelier L, Vincent A. Bone regenerate formation in cortical bone during distraction lengthening. An experimental study. *Clin Orthop.* 1990; 250:34–42. [[PubMed Citation](#)]

31. Ilizarov GA. The tension-stress effect on the genesis and growth of tissues. Part I: The influence of stability of fixation and soft-tissue preservation. *Clin Orthop.* 1989; 238:249–281. [[PubMed Citation](#)]

32. Aronson J, Shen XC, Skinner RA, Hogue WR, Badger TM, Lumpkin CK Jr. Rat model of distraction osteogenesis. *J Orthop Res.* 1997; 15:221–226. [[PubMed Citation](#)]

33. Paley D, Fleming B, Catagni M, Kristiansen T, Pope M. Mechanical evaluation of external fixators used in limb lengthening. *Clin Orthop.* 1990; 250:50–57. [[PubMed Citation](#)]

34. Li G, Simpson AH, Kenwright J, Triffitt JT. Assessment of cell proliferation in regenerating bone during distraction osteogenesis at different distraction rates. *J Orthop Res.* 1997; 15:765–772.

35. Yasui N, Sato M, Ochi T, Kimura T, Kawahata H, Kitamura Y, Nomura S. Three modes of ossification during distraction osteogenesis in the rat. *J Bone Joint Surg Br.* 1997; 79:824–830.

36. Sawaki Y, Heggie ACC. *The vascular change during and after mandibular distraction..* In: Diner PA, Vasquez MP, eds. *Second International Congress on Cranial and Facial Bone Distraction Processes.* Bologna: Monduzzi Editore SpA. 1999;23–27.

37. Li G, Simpson AH, Triffitt JT. The role of chondrocytes in intramembranous and endochondral ossification during distraction osteogenesis in the rabbit. *Calcif Tissue Int.* 1999; 64:310–317.

38. Samchukov ML, Cope JB, Harper RP. *Tissue maturation during distraction osteogenesis in bone of different embryonic origins [abstract 4]..* Paris, France: First International Congress on Cranial and Facial Bone Distraction Processes; 1997.

39. Bassett CA, Herrman I. Influence of oxygen concentration and mechanical factors on differentiation of connective tissue in vitro. *Nature.* 1961; 190:460

40. Aronson J. Temporal and spatial increases in blood flow during distraction osteogenesis. *Clin Orthop.* 1994; 301:124–131. [[PubMed Citation](#)]

41. Mosheiff R, Cordey J, Rahn BA, Perren SM, Stein H. The vascular supply to bone in distraction osteoneogenesis: an experimental study. *J Bone Joint Surg Br.* 1996; 78:497–498. [[PubMed Citation](#)]

42. Bell WH, Harper RP, Gonzalez M, Cherkashin AM, Samchukov ML. Distraction osteogenesis to widen the mandible. *Brit J Oral Maxillofac Surg.* 1997; 35:11–19.

43. Bell WH, Gonzales M, Samchukov ML, Geurrero CA. Intraoral widening and lengthening of the mandible in baboons by distraction osteogenesis. *J Oral Maxillofac Surg.* 1999; 57:548–562. [[PubMed Citation](#)]

44. Karp NS, Thorne CH, McCarthy JG, Sissons HA. Bone lengthening in the craniofacial skeleton. *Ann Plast Surg.* 1990; 24:231–237. [[PubMed Citation](#)]

45. Yanoff SR, Hulse DA, Palmer RH, Herron MR. Distraction osteogenesis using modified external fixation devices in five dogs. *Vet Surg.* 1992; 21:480–487. [[PubMed Citation](#)]

46. Glat PM, Staffenberg DA, Karp NS, Holliday RA, Steiner G, McCarthy JG. Multidimensional distraction osteogenesis: the canine zygoma. *Plast Reconstr Surg.* 1994; 94:753–758. [[PubMed Citation](#)]

47. Windhager R, Groszschmidt K, Tsuboyama T, Siegl H, Heinzl H, Seidl G, Plenk H Jr. Recorticalization after bifocal internal bone transport in the double-plated sheep femur. *J Orthop Res.* 1996; 14:94–101. [[PubMed Citation](#)]

48. Karp NS, McCarthy JG, Schreiber JS, Sissons HA, Thorne CH. Membranous bone lengthening: a serial histological study. *Ann Plast Surg.* 1992; 29:2–7. [[PubMed Citation](#)]

TABLES [Return to TOC](#)

TABLE 1. Percentage Trabecular Area in Regions of Interest

TABLE 2. Mineral Apposition Rate in Regions of Interest

FIGURES

Click on thumbnail for full-sized image.

FIGURE 1. Postoperative position of intraoral bone-borne distraction device

Click on thumbnail for full-sized image.

FIGURE 2. Regions of interest for plastic embedded sections. Three vertical by 7 horizontal ROIs (2.27 mm^2) were placed over the regenerate and adjacent host bone in order to designate areas measured for trabecular bone area and mineral apposition rate.

Click on thumbnail for full-sized image.

FIGURE 3. Reconstruction of fluorochrome images. A, Grayscale image with tetracycline emitting the brightest light; B, Grayscale image with calcein emitting the brightest light; C, Color encoded image with green representing tetracycline and orange representing calcein

Click on thumbnail for full-sized image.

FIGURE 4. Zero-week consolidation regenerate. A, Histologic section, H&E ×1; and B, Drawing illustrating that most of regenerate is occupied by fibrovascular (FV) tissue, with initial signs of bone formation (bone trabeculae—BT) at the host bone (HB) margins

Click on thumbnail for full-sized image.

FIGURE 5. Two-week consolidation regenerate. A, Histologic section demonstrating small areas of new bone formation located at the host bone (HB) margins with fibrovascular tissue (FV) in the center of the gap, Van Gieson's ×1; B, Histologic section demonstrating more advanced bone formation with regions of bony trabeculae (BT) extending up to half of the total width of the distraction gap, Attwood's ×1

Click on thumbnail for full-sized image.

FIGURE 6. Three histologic types of mandibular distraction regenerates. A, Type I—regenerate with intact interzone from superior crest

to the inferior cortex; B, Type II—regenerate with 2 dissimilar interzones. The superior aspect of the interzone is moderately wide and mostly fibrous, whereas the inferior aspect of the interzone is narrower and mostly cartilagenous when present; C, Type III—regenerate with varying degrees of interzone obliteration

Click on thumbnail for full-sized image.

FIGURE 7. Four-week consolidation regenerate. A, Histologic section demonstrating classic 3 zonal regenerate with fibrous interzone (FIZ) bounded on either side by areas of bony trabeculae (BT) originating from the host bone (HB) margins. Note that the FIZ is continuous from the superior crest to the inferior cortex, H&E ×1; B, Histologic section demonstrating more advanced bone formation with regenerate characterized by varying degrees of interzone obliteration. Note FIZ contains both fibrous tissue (FT) and cartilage tissue (CT), Attwood's ×1

Click on thumbnail for full-sized image.

FIGURE 8. Six-week consolidation regenerate. Histologic section with the interzone characterized by 2 dissimilar areas. The superior aspect of the interzone is moderately wide and mostly fibrous (FT), whereas the inferior aspect of the interzone is almost completely obliterated by bony trabeculae (BT) originating from the host bone (HB), Van Gieson's ×1

Click on thumbnail for full-sized image.

FIGURE 9. Eight-week consolidation regenerate. Histologic section of regenerate with almost complete absence of interzone. Note the presence of only host bone (HB) and regenerate bone trabeculae (BT), Attwood's ×1

[a]Clinical Assistant Professor, Department of Orthodontics; former PhD Candidate, Center for Craniofacial Research and Diagnosis, Department of Biomedical Sciences, Texas A&M University System Health Science Center—Baylor College of Dentistry; Private Practice, Dallas, Tex.

Corresponding author: Jason B. Cope, DDS, PhD, 6943 La Vista Drive, Dallas, TX 75214 (E-mail: jasoncope@orthodontist.net).

[b]Associate Director of Ilizarov Research, Department of Orthopedics, Texas Scottish Rite Hospital for Children; Assistant Professor, Department of Orthopedic Surgery, University of Texas Southwestern Medical Center; Assistant Professor, Department of Orthodontics and Department of Biomedical Sciences, Center for Craniofacial Research and Diagnosis, Texas A&M University System Health Science Center—Baylor College of Dentistry, Dallas, Tex.